IOPscience iopscience.iop.org

Home Search Collections Journals About Contact us My IOPscience

Electron paramagnetic resonance characterization of defects produced by ion implantation into silicon

This article has been downloaded from IOPscience. Please scroll down to see the full text article.

2005 J. Phys.: Condens. Matter 17 S2351

(http://iopscience.iop.org/0953-8984/17/22/024)

View the table of contents for this issue, or go to the journal homepage for more

Download details:
IP Address: 129.252.86.83
The article was downloaded on 28/05/2010 at 04:55

Please note that terms and conditions apply.

INSTITUTE OF PHYSICS PUBLISHING JOURNAL OF PHYSICS: CONDENSED MATTER

J. Phys.: Condens. Matter **17** (2005) S2351–S2360 doi:10.1088/0953-8984/17/22/024

Electron paramagnetic resonance characterization of defects produced by ion implantation into silicon

R C Barklie[1] **and C O'Raifeartaigh**[2]

[1] Physics Department, Trinity College, Dublin, Republic of Ireland
[2] Waterford Institute of Technology, Cork Road, Waterford, Republic of Ireland

E-mail: rbarklie@tcd.ie

Received 6 October 2004, in final form 12 April 2005
Published 20 May 2005
Online at stacks.iop.org/JPhysCM/17/S2351

Abstract
Many of the defects created by ion implantation into silicon can be detected by electron paramagnetic resonance (EPR). The main defects observed are isolated point defects such as Si-P3 centres (neutral 4-vacancies), silicon dangling bonds in amorphous silicon and defects associated with the so-called Σ resonance—a single broad anisotropic line; particular attention is paid to the latter defects as they have the highest population over a wide fluence range. This paper reports the effects on the nature and population of these defects of changing the fluence, mass and energy of the implanted ions as well as the effects of changing the implantation temperature.

1. Introduction

The characterization of defects formed in silicon by ion implantation has been an important area of study for many years. Since silicon, doped by ion implantation, is envisaged to remain for several more years at the heart of semiconductor device manufacture this area continues to be important. One technique that has provided much information about these defects is electron paramagnetic resonance (EPR). The pioneering work of people such as Watkins, Lee, Corbett and Brower led to the identification and characterization of a host of defects such as those listed by Sieverts [1]. In these studies the defects were usually created by electron or neutron irradiation and, as a result of the light damage, the spectra of these defects have sharp lines which makes the interpretation of the spectra easier and allows an accurate determination of the spin Hamiltonian parameters. By contrast, the EPR spectra of defects created by ion implantation tend to have broader lines and, perhaps because of this, the number of EPR studies of defects formed by ion implantation is smaller. Corbett and Karins [2] summarized in 1981 the status of our knowledge of ion-induced defects in semiconductors and included a summary of EPR measurements. Since then there have been further EPR studies such as those by Glaser *et al* [3], Waddell *et al* [4], Yajima *et al* [5], Sealy *et al* [6–8], Dvurechenskii *et al* [9], Varichenko *et al* [10], Mukashev *et al* [11], Abdullin *et al* [12], Poirier *et al* [13] and O'Raifeartaigh *et al* [14].

 © 2005 IOP Publishing Ltd Printed in the UK

One spectrum, first reported by Brower and Beezhold [15], that appeared after O^+ implantation into silicon and that had not been reported in the earlier work on neutron, proton or electron irradiated silicon is the so-called Σ spectrum. This consists of a single rather broad line that is a composite of all spectra contributing to the unresolved part of the observed spectrum, and they attributed this to defects in crystalline but heavily damaged regions of the sample. Its importance lies in the fact that its intensity exceeds that of all other spectra over a wide fluence range. Despite this importance only a rather small number of EPR reports [5–10, 14–16] refer to this spectrum. One aim of this paper is to give more attention to these Σ defects by drawing together those measurements that deal with them. The main aim is to provide a brief overview of what information EPR measurements have provided about defects produced by ion implantation into silicon and of how their nature and population is determined by the fluence, energy and mass of the ions and also by the implantation temperature.

2. Results and discussion

2.1. Dependence of defect type and population on ion fluence

The way in which the EPR spectrum of implanted silicon can vary with ion fluence is illustrated in figures 1 of the papers by Sealy *et al* [6] and O'Raifeartaigh *et al* [14]. For example, figure 1 of O'Raifeartaigh *et al* [14] shows spectra obtained for Si(111) samples implanted at 210 K with 4 MeV Ag ions; the silicon samples are n-type with resistivity of 100–150 Ω cm. At the highest fluence shown of 8.1×10^{13} Ag cm^{-2} the spectrum consists of an isotropic line with $g = 2.0056 \pm 0.0002$ and peak-to-peak linewidth, ΔB_{pp}, of 4.2 ± 0.2 G. This spectrum is characteristic of amorphous silicon [17–19] and has been attributed to silicon dangling bonds in the amorphous region—the so-called D centres. Optical reflectivity depth profiles [20] of the same samples showed that, at this fluence, an amorphous silicon layer 2.1 μm thick has been formed. This figure also shows that at the lower fluence of 1.4×10^{12} cm^{-2} the spectrum contains several sharp lines, and a comparison with the stick spectra reveals that most are associated with Si-P3 centres (planar tetravacancy [21]) and that Si-P6 may also be present; the Si-P6 centre was originally attributed to Si di-interstitials [22] but, recently, doubt was cast on this interpretation [23].The divacancy EPR spectrum is not seen because it is likely that the Fermi level is near enough to mid-gap for the divacancy to be in its diamagnetic and neutral charge state [24].

Integration of the low fluence spectrum more clearly reveals the presence of a broad spectrum first reported by Brower and Beezhold [15] and labelled the Σ spectrum. The centre of this spectrum corresponds to $g \approx 2.006$ and the width is anisotropic, being narrowest for magnetic field $B \parallel [111]$. Furthermore, the width is approximately proportional to the centre field, B_0, of the resonance: for $B \parallel [111]$ and $B_0 \approx 0.351$ T the full width at half-height $\Delta B_{1/2} \approx 1.5$ mT [14], whereas at $B_0 \approx 0.705$ T $\Delta B_{1/2} \approx 0.28$ mT [15], and this implies that a spread in g-values contributes to the linewidth. The broad but anisotropic linewidth led Brower and Beezhold [15] to attribute the Σ spectrum to point defects in heavily damaged but crystalline regions where the presence of strain and interactions between the defects broadens out separate lines into a single broad line. The location of these Σ defects in the deeper and more heavily damaged regions where the nuclear stopping power is largest was confirmed by depth profiling measurements [5, 9] that also showed that the well-defined P3 centres are mostly nearer to the surface in the more lightly damaged regions.

EPR measurements at about 9.9 GHz [14] showed that the width of the broad line starts to decrease at a sufficiently high fluence and eventually reduces to $\Delta B_{1/2} \approx 0.7$ mT corresponding to the D centre resonance. As Brower and Beezhold [15] noted, the Σ spectrum appears to

Table 1. Vacancies produced by ion implantation into silicon.

Ref.	Ion	T_i	Fluence (cm^{-2})	V_2 (cm^{-2})	V_4 (cm^{-2})	$\sum$ (cm^{-2})	Vacancy/ion EPR	Vacancy/ion TRIM 96[a]
[15]	160 keV O^+	Room temp.	2×10^{12}	1.4×10^{14}	1.4×10^{14}	2.6×10^{14}	680	901
[15][b]	160 keV O^+	Room temp.	2×10^{12}	—	5×10^{12}	5×10^{13}	28	901
[16]	140 keV B^+	Room temp.	2×10^{13}	—	4×10^{12}	6.6×10^{13}	7	527
[7]	2 MeV Si^+	LN	1×10^{13}	—	3.5×10^{12}	4×10^{13}	9.2	4 833
[7]	3 MeV Au^+	LN	1×10^{12}	—	3×10^{12}	6×10^{13}	132	27 708
[14]	4 MeV Ag^+	210 K	7×10^{11}	—	2.4×10^{12}	3×10^{13}	95	23 608
[8]	1.5 MeV Si^+	Room temp.	1×10^{13}	—	2×10^{12}	1.6×10^{13}	3	4 609
[8]	50 keV Si^+	Room temp.	1×10^{13}	—	—	6×10^{12}	1	692
[8]	50 keV B^+	Room temp.	5×10^{13}	—	3.5×10^{11}	8×10^{12}	0.4	322

[a] Taking the displacement energy as 15 eV.
[b] Implantation into heavily doped n-type Si: all other samples are lightly doped Si.

degenerate into the D centre resonance. The authors were unable to separate unambiguously the X-band broad line spectrum into its Σ and D components and so just plotted the total areal spin concentration (i.e. spin population per unit implanted area) of Σ + D centres versus fluence. However, as noted above, in the 10^{12} Ag cm^{-2} fluence region the Σ defects dominate whereas the D centres dominate in the 10^{14} Ag cm^{-2} region. Thus figure 3 of O'Raifeartaigh *et al* [14] shows that in the 10^{12} Ag cm^{-2} region the Σ defects increase almost linearly with fluence. Such a result was also found by Brower and Beezhold [15] who measured the defects created by the room temperature implantation into intrinsic silicon of 160 keV O^+. They were able to separate the Σ and D contributions, probably because the measurements were made at a higher magnetic field, and found that for fluences $\leqslant 10^{13}$ O^+ cm^{-2} the Σ defect population increases nearly linearly with fluence; they found that this population reaches a maximum and then decreases as the D centre population increases.

Figure 3 of O'Raifeartaigh *et al* [14] also shows that the P3 areal concentration increases to a maximum and then starts to decrease, presumably because these defects are gradually incorporated into more complex defects as the damage level rises. A similar dependence of the nature and population of defects on ion fluence has been reported for implantations of B [8, 16, 18], Si [5, 6, 8], P [5, 18] and Au [6].

As well as their results mentioned above, Brower and Beezhold [15] examined the defects formed by the room-temperature implantation of 160 keV O^+ into heavily doped n-type silicon. In this case Si-G7 (negative divacancies) and Si-S2 centres (suggested to be the negative charge state of the 4-vacancy) were observed as well as the Σ and D defects. However, once again, in the fluence range 5×10^{11}–5×10^{14} O^+ cm^{-2} the Σ defects have the largest areal concentration. In view of the dominance of these defects over a wide fluence range it is unfortunate that so little is known about them. Since at that time no single silicon interstitials had been observed and since the vacancy is mobile below room temperature and combines with other vacancies or impurities, Brower and Beezhold [15] assumed that there are at least two vacancies on average per Σ centre. Taking the lower limit of two it is interesting to evaluate the total number of vacancies per ion associated with EPR detected centres. Table 1 shows that for the case of 160 keV O^+ implanted into heavily doped n-type silicon the number of these vacancies per ion is a high proportion of that given by TRIM 96 (with displacement energy of 15 eV), but that when the silicon is lightly doped the number is much less than the total given by TRIM 96. This difference may be because when the Fermi level is near mid-gap then not only the divacancies but also a significant proportion of the Σ defects are in a diamagnetic state. It is worth noting

however that the trends exhibited by the EPR active defects are the same for implantation into both lightly and heavily doped (n-type) silicon.

One further question concerning the Σ defects is whether they are created in previously undamaged silicon or only in regions where damage cascades overlap. Yajima *et al* [5] successfully fitted the dependence of the Σ defect concentration (referred to in their paper as 'indefinite point defects') on the fluence of 3 MeV phosphorus and silicon ions implanted at about room temperature in the range 3×10^{12}–10^{14} cm^{-2}. In their model the Σ defects were assumed to occur only in heavily damaged regions formed by the overlap of one or more lightly damaged regions. On the other hand, as pointed out by Brower and Beezhold [15], the linear growth of the Σ spectrum at low fluences observed by them for 160 keV O^+ implantation—and by others [6] for both Si and Au implants—suggests that they can be formed in previously undamaged regions even for the implantation of ions as light as O^+. This question is therefore not resolved. What is certain is that they are predominantly in the more heavily damaged regions where the nuclear stopping power is highest, unlike the isolated point defects such as Si-P3 centres that are located in the more lightly damaged regions closer to the surface. It is interesting to note that Karmouch *et al* [25] found evidence for the presence of highly disordered zones generated by each implantation cascade; the evidence came from measuring the heat released on annealing silicon implanted at room temperature with 30 keV Si^-, 15 keV Si^- and 15 keV C^-. It is plausible that at least some of these highly disordered zones contain defects associated with the Σ spectrum.

2.2. *The effect of changing the ion energy*

Figure 1 shows the EPR spectrum of silicon implanted with 1.5 MeV and 50 keV Si^+ to a fluence of 1×10^{13} cm^{-2} and 2×10^{13} cm^{-2} respectively. Float zone, n-type, 500–1000 Ω cm (001) silicon wafers were implanted at room temperature and, to prevent appreciable substrate heating, fluence rates lower than 3×10^{11} ions cm^{-2} s^{-1} were used [8]. Analysis of these spectra shows that the ratio of the populations of Si-P3 to $\Sigma + D$ is much higher for the 1.5 MeV implanted sample than for the 50 keV implant. Figure 2 shows how the areal concentrations of these defects vary with fluence for the above implants and also for the implantation of 0.7 MeV Si^+; the concentration of Si-P3 defects in the 50 keV implanted sample is always $\leqslant 3 \times 10^{11}$ cm^{-2}. There is no significant difference between the $\Sigma + D$ concentrations for the 1.5 and 0.7 MeV implants and in the fluence range 7×10^{12}–2×10^{14} cm^{-2} their concentration ranges from 3 to 5 times larger than at the corresponding fluence of the 50 keV implant. However, the Si-P3 areal concentrations after 0.7 MeV and 50 keV implantations are lower by about a factor of 2 and by more than a factor of 20 respectively compared to their concentration after the 1.5 MeV implantation. Thus, in the case of the two spectra shown in figure 1, the effect of changing the implantation parameters from 50 keV, 2×10^{13} cm^{-2} to 1.5 MeV, 1×10^{13} cm^{-2} is to increase the $\Sigma + D$ and Si-P3 concentrations by about $\times 3$ and by $> \times 20$ respectively so that the effect of the increasing the ion energy from 50 keV to 1.5 MeV is to increase the ratio of the populations of Si-P3 to $\Sigma + D$. To what extent can TRIM 96 account for these differences? TRIM 96 gives the ratio of the total number of vacancies per ion for implants at 1.5 MeV, 0.7 MeV and 50 keV to be about 1:0.82:0.15, and this is similar to the corresponding $\Sigma + D$ population ratios of 1:1:(0.2–0.3). Since most of the vacancies are created where the nuclear stopping power is greatest, this result is consistent with the location of these defects in the more heavily damaged regions. On the other hand, the Si-P3 areal concentrations ratio of 1:0.5:$<$0.05 is very different to the above vacancy ratio but closer to the ratio of the ion energies of 1:0.47:0.033. Since, as figure 3 shows, the extent of the more lightly damaged regions at lower stopping power increases almost in proportion of the ion energy, this result is also consistent with the idea that the Si-P3 defects are in such a region.

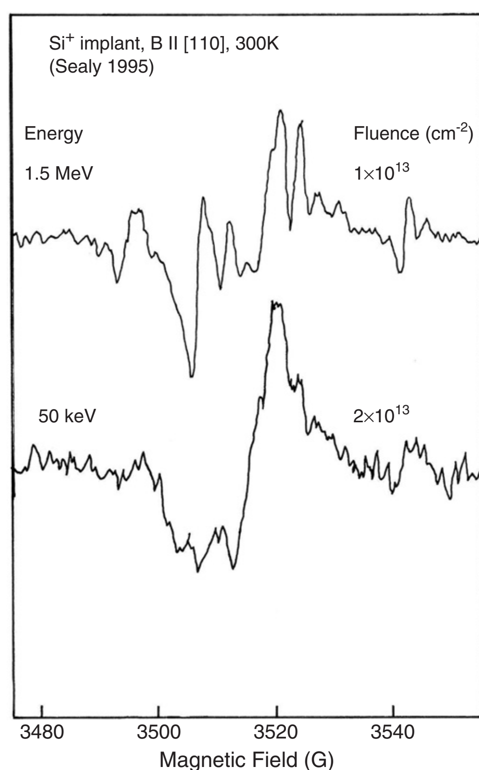

Figure 1. EPR spectra of silicon implanted at room temperature with Si^+ ions of energy 1.5 MeV or 50 keV.

2.3. The effect of changing the ion mass

Figure 4 shows EPR spectra obtained for the implantation of 2 MeV $^{28}Si^+$ and 3 MeV $^{197}Au^+$; the implantations were at liquid nitrogen (LN) temperature into (100) float zone, p-type Si wafers of resistivity 150 Ω cm [6]. What is striking about the figure is that the spectra obtained and the way they change with fluence are almost identical for the Si^+ and Au^+ implantations even though the ion masses are so different. Figure 5 reinforces this point by showing that an approximate coincidence of the Si^+ and Au^+ data points would occur if the Au^+ data points were shifted along the fluence axis by an amount corresponding to an increase in fluence by a factor of between 10 and 20. Once again the $\Sigma + D$ areal concentration is dominated by the Σ defects at the lowest fluence and by the D centres at the highest fluence for both Si and Au ions. Not surprisingly, the implantation of ions of different mass at about room temperature gives rise to similar behaviour, as shown in figure 6. To what extent can these shifts be accounted for by the predictions of TRIM 96? This gives about 28 000 total vacancies per 3 MeV Au^+ ion, which is about 6 times larger than the corresponding figure of about 4800 for 2 MeV Si^+, and figure 7 shows that the maximum number of vacancies/ion/nm is about 10 times higher for the Au implantation. Since the Σ and D centres are mostly formed where the nuclear stopping power is highest, this would suggest that a given $\Sigma + D$ areal concentration requires a 2 MeV Si^+ fluence of between about 6 and 10 times larger than that of 3 MeV Au^+, and this agrees roughly with what is observed. The same reasoning would suggest that a given $\Sigma + D$ areal concentration produced by implanting 1.5 MeV Si^+ would require a fluence larger by

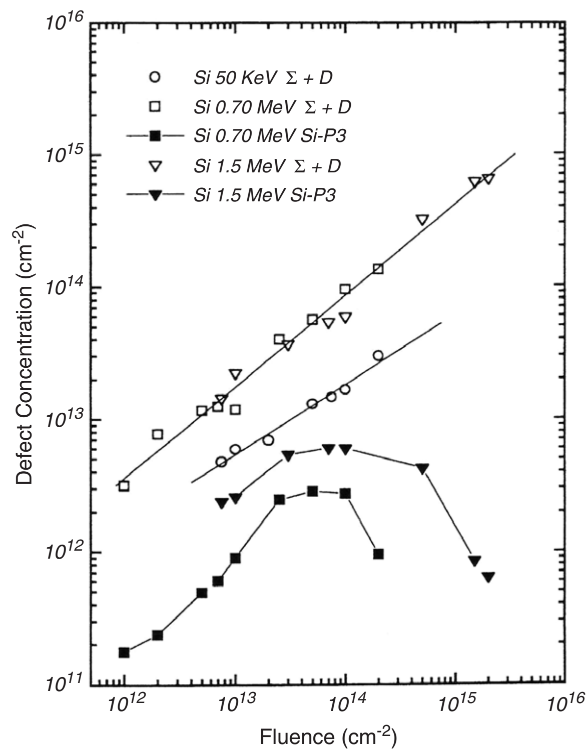

Figure 2. The fluence dependence of the areal concentration of Si-P3 and Σ/D centres produced by the room-temperature implantation of 50 keV, 0.70 keV or 1.5 MeV Si^+ ions.

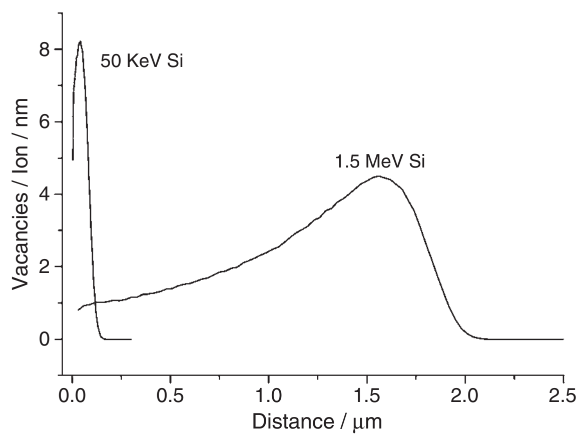

Figure 3. TRIM 96 evaluation of the total vacancies/ion/nm versus depth for the implantation into silicon of 50 keV or 1.5 MeV Si^+.

between 4 and 5 times that of a 4 MeV Ag implantation, but this is considerably smaller than the measured factor of about 30; however, this difference may be related to the increase in defect recombination that will occur at the higher implantation temperatures.

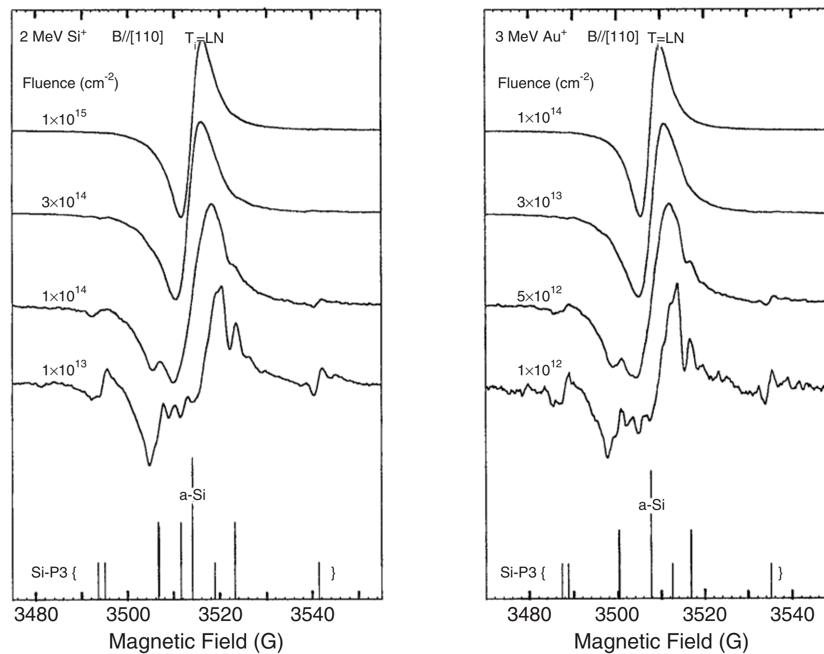

Figure 4. EPR spectra of Si implanted at LN temperature with either 3 MeV $^{197}Au^+$ or 2 MeV $^{28}Si^+$.

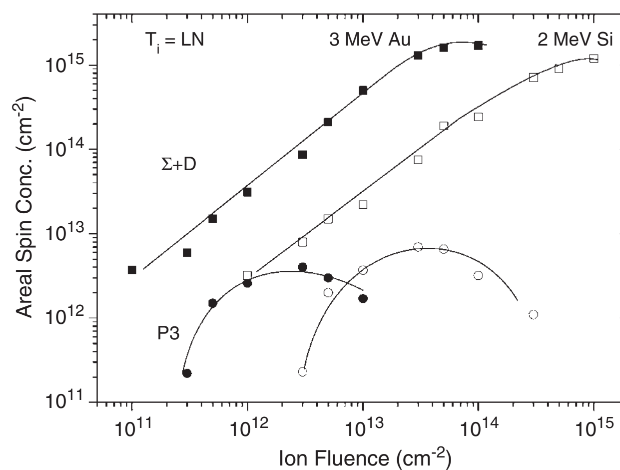

Figure 5. The fluence dependence of the areal concentrations of Si-P3 and Σ/D centres produced in silicon by the implantation at LN temperature of 3 MeV $^{197}Au^+$ or 2 MeV $^{28}Si^+$.

2.4. The effect of changing the implantation temperature

Figure 8 compares spectra of samples implanted with 4 MeV Ag^+ at different temperatures, T_i. The low fluence spectra have the same shape at each T_i and the way they, and hence also the defects, change with increasing fluence is similar. Also similar is the way in which the width of the broad $\Sigma + D$ line changes with fluence; however, the onset of the decrease in width shifts to higher fluence as T_i increases, and rate of decrease of width with increasing

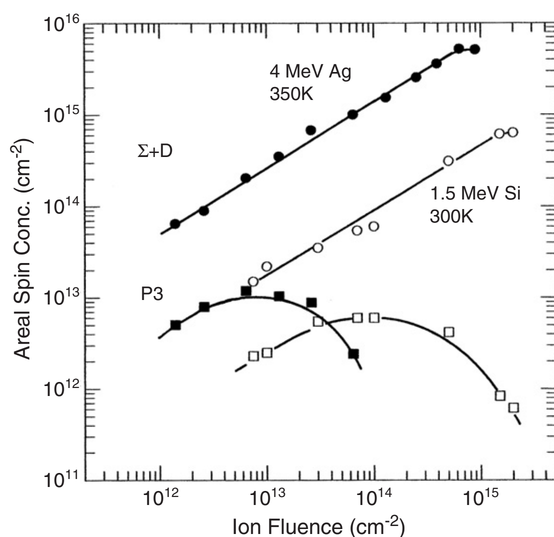

Figure 6. The fluence dependence of the areal concentrations of Si-P3 and Σ/D centres produced in silicon by the implantation of 4 MeV $^{108}Ag^{+}$ at 350 K or 1.5 MeV $^{28}Si^{+}$ at 300 K.

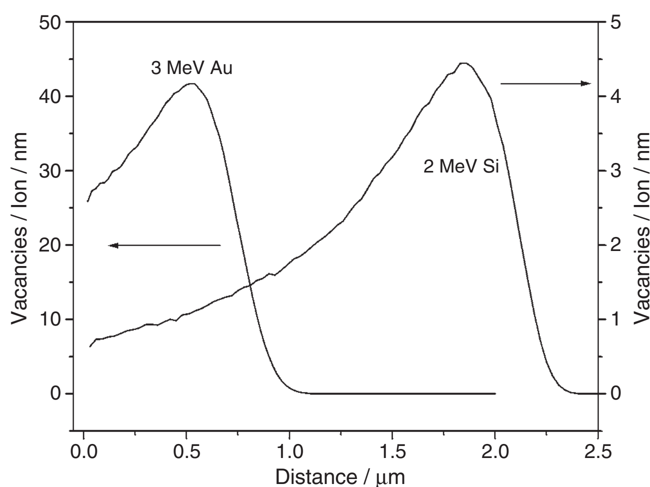

Figure 7. TRIM 96 evaluation of the total vacancies/ion/nm versus depth for the implantation into silicon of 3 MeV Au^{+} or 2 MeV Si^{+}.

fluence, in the transition region, is decreased [14]. Also decreased with increasing T_i is the rate of increase of the $\Sigma + D$ areal concentration with increasing fluence [14]. These changes reflect the expected increase in recombination of defects as T_i is raised. Of course, EPR only gives the integral over depth of the volume concentration of defects, and the dependence of this on fluence will vary with depth as shown, for example, by the depth profiling of damage carried out by Lindner *et al* [20].

At sufficiently high implantation temperature the spectrum of the Si-P3 4-vacancy centre is replaced by that of the Si-P1 5-vacancy centre [6].

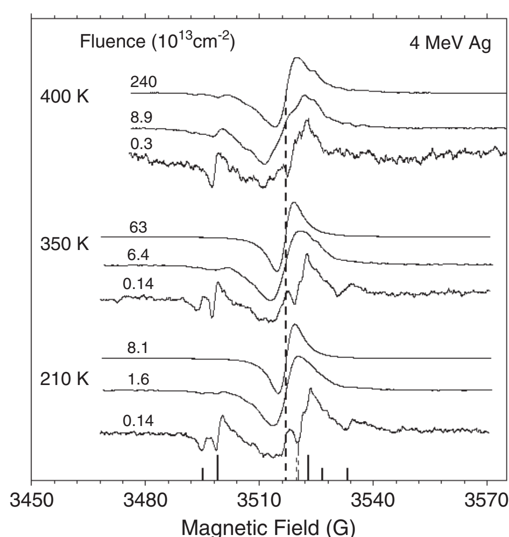

Figure 8. The fluence dependence of EPR spectra ($B \parallel [111]$) of Si implanted with 4 MeV Ag^+ at 210, 350 or 400 K.

3. Conclusions

The results presented in this paper show that the same types of defect are detected by EPR for the implantation into silicon of ions with a wide range of masses, energies and implantation temperatures. For all ions at sufficiently low fluence the defects are point defects such as the Si-P3 centres in the more lightly damaged regions and the Σ centres in the more heavily damaged regions. Increasing the fluence causes an initial increase and then decrease in the Si-P3 population and may lead to the eventual degeneration of the Σ centres into Si-D centres. Increasing the ion energy tends to increase the ratio of the Si-P3 to Σ defect areal concentrations. Increasing the ion mass reduces the fluence at which a given areal defect concentration occurs. As the implementation temperature is raised then a higher implantation fluence is required to produce a given defect areal concentration, and there is a reduction in the fluence rate of change of these concentrations.

Acknowledgments

We are very grateful to Drs W L Brown and D C Jacobson (Bell Laboratories, Murray Hill) for the 3 MeV Au^+ and 2 MeV Si^+ implanted samples, to Drs G Lulli and R Nipoti (CNR-Istituto LAMEL) for the samples implanted with 50 keV, 700 keV and 1.5 MeV Si^+ and to J K N Lindner for the supply of the 4 MeV Ag^+ implanted silicon. We thank Dr B J Jones for help with preparing the manuscript.

References

[1] Sieverts E G 1983 *Phys. Status Solidi* b **120** 11
[2] Corbett J W and Karins J P 1981 *Nucl. Instrum. Methods* **182/183** 457
[3] Glaser E, Gotz G, Sobolev N and Wesch W 1982 *Phys. Status Solidi* a **69** 603
[4] Waddell C N, Spitzer W G, Fredrickson J E, Hubber G K and Kennedy T A 1984 *J. Appl. Phys.* **55** 4361

[5] Yajima Y, Natsuaki N, Yokogawa K and Nishimatsu S 1991 *Nucl. Instrum. Methods* B **55** 607
[6] Sealy L, Barklie R C, Reeson K J, Brown W L and Jacobson D C 1992 *Nucl. Instrum. Methods* B **62** 384
[7] Sealy L, Barklie R C, Brown W L and Jacobson D C 1993 *Nucl. Instrum. Methods* B **80/81** 528
[8] Sealy L, Barklie R C, Lulli G, Nipoti R, Balboni R, Milita S and Servidori M 1995 *Nucl. Instrum. Methods* B **96** 215
[9] Dvurechenskii A V, Karanovich A A and Rybin A V 1993 *Nucl. Instrum. Methods* B **80/81** 620
[10] Varichenko V S, Zaitsev A M, Lindner J K N, Domres R, Penina N M, Erchak D P, Chelyadinskii A R and Martinovitsh V A 1994 *Nucl. Instrum. Methods* B **94** 240
[11] Mukashev B N, Abdullin K A and Gorelkinskii Y V 1988 *Phys. Status Solidi* a **168** 73
[12] Abdullin K A, Mukashev B N and Gorelkinskii Y V 1996 *Semicond. Sci. Technol.* **11** 1696
[13] Poirier R, Avalos V, Dannefaer S, Schiettekatte F, Roorda S and Misra S K 2003 *Physica* B **340–342** 752
[14] O'Raifeartaigh C, Barklie R C and Lindner J K N 2004 *Nucl. Instrum. Methods* B **217** 442
[15] Brower K L and Beezhold W 1972 *J. Appl. Phys.* **43** 3499
[16] Beezhold W and Brower K L 1973 *IEEE Trans. Nucl. Sci.* **20** 209
[17] Morehead F F, Crowder B L and Title R S 1972 *J. Appl. Phys.* **43** 1112
[18] Sobolev N A, Gotz G, Karthe W and Schnabel B 1979 *Radiat. Eff.* **42** 23
[19] Thomas P A, Brodsky M H, Kaplan D and Lepine D 1978 *Phys. Rev.* B **18** 3059
[20] Lindner J K N, Eder J and Stritzker B 1999 *Mater. Res. Soc. Symp. Proc.* **540** 31
[21] Brower K L 1971 *Radiat. Eff.* **8** 213
[22] Lee Y H, Gerasimenko N N and Corbett J W 1976 *Phys. Rev.* B **14** 4506
[23] Jones R, Eberlein T A G, Pinho N, Coomer B J, Goss J P, Briddon P R and Oberg S 2002 *Nucl. Instrum. Methods* B **186** 10
[24] Brower K L, Vook F L and Borders J A 1969 *Appl. Phys. Lett.* **15** 208
[25] Karmouch R, Mercure J-F, Anahory Y and Schiettekatte F 2005 *Appl. Phys. Lett.* **86** 031912